Laser-Based In Situ Techniques: Novel Methods for Generating Extreme Conditions in TEM Samples

MITRA L. TAHERI,[1]* THOMAS LAGRANGE,[1] BRYAN W. REED,[1] MICHAEL R. ARMSTRONG,[1] GEOFFREY H. CAMPBELL,[1] WILLIAM J. DEHOPE,[1] JUDY S. KIM,[1,2] WAYNE E. KING,[1] DANIEL J. MASIEL,[2] AND NIGEL D. BROWNING[1,2]
[1]*Chemistry, Materials, Earth & Life Sciences Directorate, Lawrence Livermore National Laboratory, Livermore, California*
[2]*Department of Chemical Engineering & Materials Science, University of California-Davis, Davis, California*

KEY WORDS in situ; laser; transmission electron microscopy; dynamic; transformation; growth

ABSTRACT The dynamic transmission electron microscope (DTEM) is introduced as a novel tool for in situ processing of materials. Examples of various types of dynamic studies outline the advantages and differences of laser-based heating in the DTEM in comparison to conventional (resistive) heating in situ TEM methods. We demonstrate various unique capabilities of the drive laser, namely, in situ processing of nanoscale materials, rapid and high temperature phase transformations, and controlled thermal activation of materials. These experiments would otherwise be impossible without the use of the DTEM drive laser. Thus, the potential of the DTEM as a new technique to process and characterize the growth of a myriad of micro and nanostructures is demonstrated. *Microsc. Res. Tech. 72:122–130, 2009.* Published 2009 Wiley-Liss, Inc.†

INTRODUCTION

Recent years have seen a dramatic growth in capabilities for in situ studies of materials dynamics in a transmission electron microscope (TEM). In situ TEM experienced great expansion when some of the early in situ TEM experiments were designed for high voltage electron microscopes (HVEMs), and dated back to as early as the1950s and1960s (Brown et al., 1973; Caillard and Martin, 1982, 1983; Hale and Butler, 1981; Vogelsang et al., 1986). These experiments involved the study of dislocation dynamics during creep, recovery processes, electron irradiation, and other aspects of microstructural evolution under stress, strain, or heat. These experiments required special in situ stages that could apply the desired microstructure-changing effect (e.g., strain). In later years, in situ TEM became popular in other fields, such as surface science and catalysis (Bovin et al., 1985; Datye, 2003; Sinclair et al., 1981; Smith and Marks, 1985; Wallenberg et al., 1985, 1986). With this came the advent of early environmental cell stages, ultra high vacuum in situ TEM experiments, and finally, the development of the environmental TEM (Gai, 2002; Sharma and Weiss, 1998). As the technique matured, in situ TEM experiments become more adventurous, including complex capabilities such as simultaneous biasing, indentation, and fluid interaction. Perhaps the most prevalent in situ TEM technique is the oldest form: in situ heating/annealing (with a resistive heating stage in which the entire sample is heated uniformly). Most materials TEM facilities include sample heating capabilities, since thermally activated microstructural evolution processes are the backbone of materials science. These processes include nucleation and growth, recrystallization and grain growth, phase transformations, and dislocation motion.

Though in situ heating in a TEM has provided a wealth of information with respect to microstructural evolution (Gleiter, 1969; Merkle et al., 2004; Rae and Smith, 1980; Rae, 1981; DA Smith et al., 1980; Taheri et al., 2004), the technique has fundamental limitations, due to the nature of resistive, or joule, heating. A typical in situ heating stage will heat the entire sample, along with part of the stage, by passing current through a coil of fine wire placed very close to the sample. The relatively large volume of heated material leads to substantial thermal drift of the sample position, which adversely affects imaging. The temperature is measured with a thermocouple placed very close to the sample, but the exact temperature of the sample itself is difficult to determine precisely, especially for low-conductivity materials. The sample temperature may take several minutes to ramp up and stabilize, which makes it difficult to study very fast processes particularly when the processes of interest are competing with slower processes such as oxidation or sublimation (examples shown below). The maximum temperature is limited to ~1500 K or less by the coil design and the materials used in the construction of the sample holder. Furthermore, it is typically impossible to heat only a small region of the sample. This can be a problem for the study of irreversible processes (e.g., recrystallization and grain growth), particularly when sample preparation is difficult or expensive, since an entire sample must be consumed for each measurement. Also,

*Correspondence to: Mitra L. Taheri, Department of Materials Science & Engineering, Drexel University, Philadelphia, PA, USA. E-mail: mtaheri@coe.drexel.edu

Received 28 February 2008; accepted in revised form 7 July 2008
DOI 10.1002/jemt.20664
Published online 22 January 2009 in Wiley InterScience (www.interscience.wiley.com).

processes that involve large spatiotemporal temperature gradients (e.g., cell formation in rapid solidification) are very difficult to study using conventional in situ TEM.

To overcome the above-mentioned deficiencies of conventional in situ heating experiments, temperature changes and heating should be site-specific and localized to the region of interest, reducing temperature constraints and minimizing thermal drift problems. In order to study fast processes, the method should also provide high heating rates as well as high temperatures. Laser-based techniques can provide such conditions, with heating rates limited only by the intensity of the laser ($>10^{16}$ K/s) and temperature limits that depend on the available laser energy and laser-material interactions. The obvious caveats to the laser-based method are that laser-material interactions must be modeled, and the laser system must be flexible, i.e., optical properties differ in materials requiring that the laser wavelength be tunable and matched to the sample material's absorption characteristics. If modeled well, the temperatures can be controlled precisely in a localized region. Moreover, lasers can provide conditions that control more than just heating; they can be used to induce high pressures in the sample, photo-excitations, produce vapor-condensate reactions by laser ablation, etc. In situ laser irradiation allows the study of a host of materials processes and new and interesting in situ experiments that are not accessible with standard in situ techniques.

In this article, a novel method for treating a sample with a laser to study thermally activated microstructural processes is presented. This method is incorporated into a larger instrument, the dynamic TEM (DTEM), in which laser pulsed photoemission of electrons is used to achieve high (nanosecond) temporal resolution. The DTEM utilizes a "pump-probe" style experiment methodology, whereby one laser hits the sample to initiate a reaction, and another laser hits the electron source to image the reaction. In this article we will concentrate on how the use of a laser to treat samples differs greatly from a heating stage. Specifically, we discuss the advantages of the laser over conventional resistive heating methods, and discuss various applications and recent results.

MATERIALS AND METHODS

In recent years, interest in ultrafast in situ TEM has increased dramatically, from stroboscopic (Lobastov et al., 2005; Zewail, 2005) to pump-probe single shot methods (Bostanjoglo, 2002; Dömer and Bostanjoglo, 2003; King et al., 2005, 2006; Lagrange et al., 2006, 2007). Our group at Lawrence Livermore National Laboratory has led the current effort in single-shot in situ TEM with the successful design and development of the DTEM. The DTEM, schematically shown in Figure 1, consists of a TEM column (JEOL 2000FX) to which two pulsed lasers have been added. One laser, a 15-ns-duration frequency-quintupled Nd:YLF, enables electron beam imaging operation in a pulsed photoemission mode (the microscope can also operate using conventional thermionic continuous-wave (CW) mode). The pulsed mode's nanosecond-scale imaging capability greatly exceeds the ~30 Hz time resolution of conventional in situ TEM dictated by video rate recording techniques and has the potential to provide a detailed understanding of materials processes. A second, Nd:YAG pulsed laser, labeled "hydro-drive laser" in Figure 1, is incident directly on the sample.

The laser pulse is used to initiate a transient process to be investigated, e.g., phase transformation or chemical reactions. The stimulation of the process can be precisely timed with the electron probe, and thus a series of 15 ns, "snap-shot" images can be taken at selected delays between the pump and probe. Though the DTEM has proven to be useful for ultrafast imaging and characterization (King et al., 2006; Lagrange et al., 2006, 2007), in this article, we show the function of the DTEM as a new tool for in situ TEM studies of thermally activated materials processes.

The use of a laser to treat a sample is not at all similar to resistive heating. Resistive heating is slow (with a typical time scale of seconds to minutes) and heats the entire sample roughly uniformly to a temperature measured with a nearby thermocouple. Laser treatment instead delivers a pulse of nonthermal energy that is highly confined in space and time. This enables unique experiments involving very rapid processes, very high spatiotemporal temperature gradients, and nonequilibrium processes such as pulsed laser ablation.

We have implemented various Nd:YAG laser systems for specimen drive that have FWHM pulse duration ranging from 3 to 8 ns. The laser pulse has a Gaussian energy spatial and temporal distribution, and the size of the laser spot depends on the laser beam mode quality and wavelength and the numerical aperture of the lens system. On average for 1064 nm laser pulses, the $1/e^2$ diameter is ~150 μm, and at shorter wavelengths, e.g., 355 nm, the laser beam diameter is ~50 μm. The fundamental wavelength (1064 nm) can be adjusted using nonlinear harmonic generation crystals, e.g., the 1064 nm laser beam can be converted to 532 or 355 nm wavelengths, depending on the absorption characteristic of the sample and the desired experimental conditions. The pulse energy can be precisely controlled over a very wide range (from nanojoules to millijoules, enabling anything from gentle heating to instant ablation), but the temperature of the treated region can be determined only with some effort, and only indirectly. The temperature is a rapidly varying function of space and time, and precise temperature measurements of micrometer-sized regions on μs time scales are extremely difficult with any existing technology. Instead the temperature is determined by a combination of modeling and identification of known calibration points. The laser wavelength and incident angle, and the thickness and complex dielectric function (or the measured absorptivity) of the sample, allow a calculation of the absorbed energy per unit area during the pulse. Dividing by the sample's heat capacity per unit area yields the temperature rise for a given laser intensity. We can then predict the pulse energy required to reach an experimentally identifiable state (e.g., the melting point, easily detected by a loss of crystalline order in the time-resolved diffraction pattern) and verify this threshold experimentally to produce a final calibration of the model. Having three different laser wavelengths available (1064, 532 and 355 nm) improves our ability to optimize the sample drive for the absorption character-

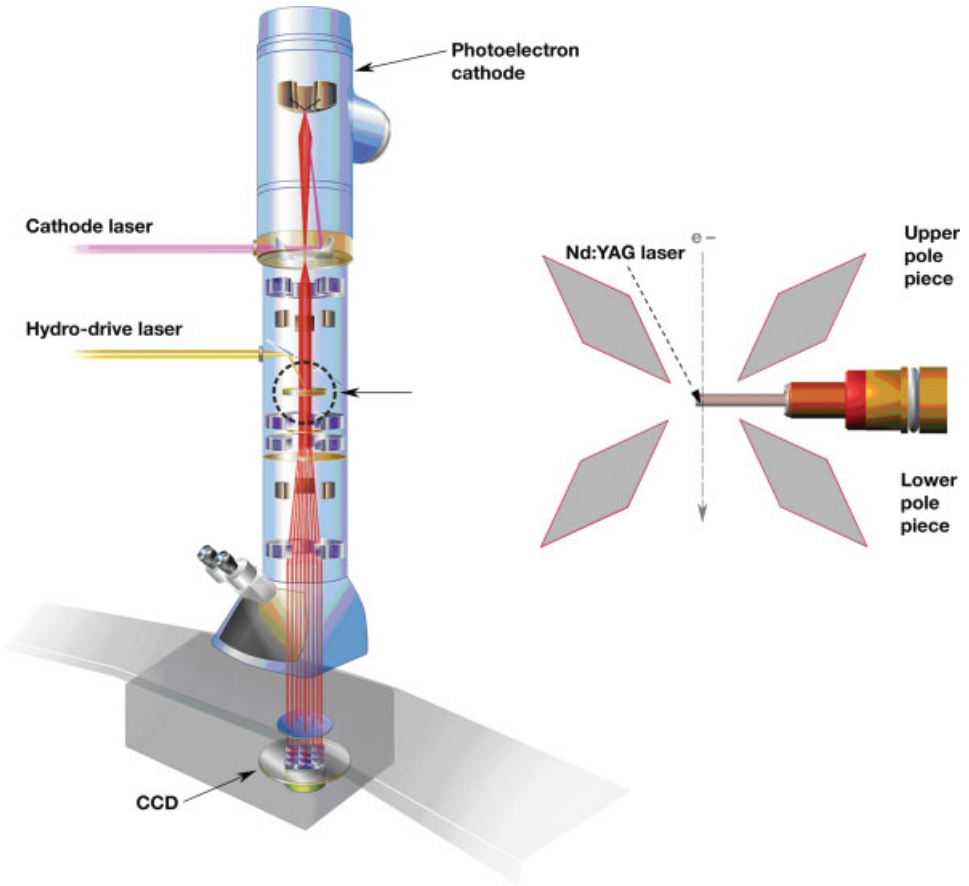

Fig. 1. Schematic diagram of the DTEM column. The sample region is circled, showing where the drive laser treats the sample, hitting it at an incident angle of ~43°. [Color figure can be viewed in the online issue, which is available at www.interscience.wiley.com.]

istics of each sample. For much higher intensities, particularly those approaching or exceeding the sample's ablation threshold, the simple linear absorption model is irrelevant and much more complex modeling is required if the sample temperature must be known.

To be more precise, this calculated temperature rise only applies on an intermediate time scale, long enough after the laser pulse for thermal equilibration in the foil-normal direction but short enough that lateral diffusion is negligible. Fortunately, these two time scales are of convenient and highly distinct magnitudes. If we postulate a typical thermal diffusivity of order $D = 10^{-5}$ m^2/s, then a $d = 100$ nm thick sample will equilibrate in the normal direction on a time scale of order $d^2/D \sim 1$ ns, which is less than the laser pulse duration. The time scale for lateral diffusion is determined by the same formula but with d set equal to the size of the laser spot, ~50 μm, which comes to 250 μs. So for many experiments the sample temperature can be taken to be constant over the DTEM's typical time scale of 10 ns to 10 μs. For comparison, on the 30 ms video frame time of conventional in situ TEM, an entire DTEM pump-probe experiment including cooling of the sample to ambient temperature can take place between two frames of video.

RESULTS

In this section, results from drive laser experiments are presented with the improvement or unique benefit that each experiment revealed over conventional resistive heating in situ TEM. These examples highlight the ability of the drive laser to go beyond resistive heating in temperature, heating (thus transformation) rate, and heat distribution (the ability to target specific regions).

Rapid and Controlled Heating Experiments

Our recent studies on the martensitic phase transformations in Ti, namely the α to β transition, benefit from the unique in situ laser drive capabilities in DTEM (Lagrange et al., 2007). Since the structural change in this transition occurs by a diffusionless mechanism that is accomplished by cooperative atomic shuffles, phase boundaries move at high velocities, approaching 1/3 the speed of sound. Due to the innate speed of these interfaces, experimental observation of their structure and even of the overall transformation kinetics has been difficult. To effectively study the nucleation and growth behavior of these transformations, the heating rates must be high ($>10^{10}$ K/s) and

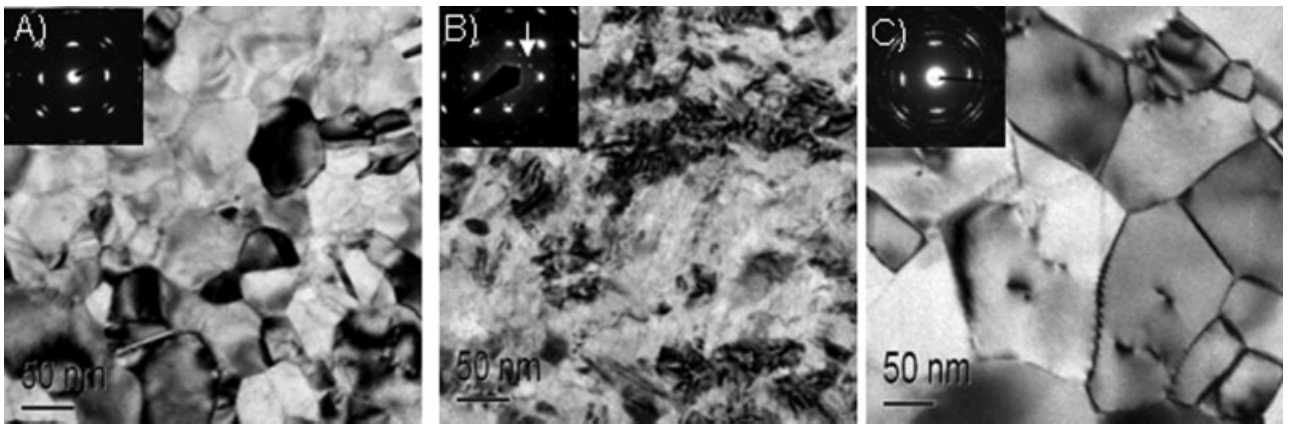

Fig. 2. Brightfield TEM images of nanocrystalline Ti film microstructure (**A**) before and (**B**) after heating to above 800K. The satellite diffraction spots in the inset SAED pattern in (B) (indicated by the arrow) indicate formation of TiN and TiO_x phases due to reactions with residual oxygen and nitrogen in TEM in vacuum system. (**C**) After one laser heating pulse (estimated maximum temperature ~1800 K).

the time resolution of the observation technique must be such as to capture a "snap-shot" image of the transient phase evolution. Moreover, the technique must also allow for heating of the specimen in the range of temperatures associated with the transformation, between 1150 and 1925 K. Most resistive-type heating holders are limited to temperatures below ~1575 K and heating rates of ~10 K/s and are thus unable to study kinetics in these materials. However, using pulsed laser irradiation, high temperatures and heating rates (10^{11} K/s) are easily obtainable, where Ti TEM foils can be melted or even vaporized within a few nanoseconds.

The greatest limitation for studying the rapid α-phase to β-phase transition in Ti with standard in situ heating techniques is the concomitant chemical reactions that occur at high temperatures with residual gases in the TEM vacuum. Figure 2 illustrates the degradation and microstructural changes after heating for a short period (1 min) above 800 K (temperatures below 1150 K transition temperature). The microstructure of the heat-treated film (Fig. 2B) is vastly different from the initial microstructure (Fig. 2A). The grain structure is no longer distinct and is more refined. The numerous Moiré fringes and satellite spots in the selected-area electron diffraction (SAED) pattern indicate the formation of secondary oxide and nitride phases (most likely on the surface). The laser-treated films however (Fig. 2C) do not exhibit such microstructural changes. Instead, significant grain growth is observed, and no additional phases are detected in the SAED patterns, indicating that chemical reactions were kinetically limited by rapid heating and cooling rates. Oxygen and nitrogen are both α-phase stabilizers, and even at ppm levels, these elements have a great effect on martensitic transformation kinetics. In fact, the transformation to β-phase was never observed in films heated with resistive-type heating holders, even with prolonged heating (>5 min) to temperatures (~1250 K) above the transition temperature (1153 K). These compositional and microstructural changes can be expected with prolonged heating, even at vacuum pressures of 10^{-7} Torr, due to the reactive nature of Ti, the large surface area and nanocrystalline microstructure of the films. Using an ultrahigh vacuum system may help to prevent oxidation and nitride formation, but the limitations on heating rates and maximum temperature of standard heating holders still do not allow the study of these transformations in Ti.

Unique Laser-Based Experimental Processing Techniques

Not only is the drive laser used to simply initiate a reaction, but also, it can be used to perform in situ experiments otherwise impossible in conventional TEM instruments. Previous use of a pulsed laser in a TEM to treat thin films was explored by Bostanjoglo and coworkers (Bostanjoglo and Nink, 1996; Bostanjogo and Weingartner, 1997; Bostanjoglo et al., 1991, 1994). Some of the most useful applications of the drive laser are in nanotechnology. For instance, the processing of nanoscale structures and devices requires the high energy, high temperature, and site specific heating capabilities of the DTEM drive laser. Below are two examples of the utility of the drive laser in nanotechnology.

Laser Ablation Synthesis of Nanowires. We have shown that the DTEM can be used to fabricate crystalline nanowires (NWs). Critical to the efficient development of nanoscale electronic devices is the understanding and control of the initial nucleation and growth stages (how the building blocks form their foundation). The origin of texture, morphology, and extended defects in nanostructures during nucleation and growth is crucial to their future use in device fabrication. One approach to NW growth is hybrid pulsed-laser ablation/chemical vapor deposition (PLA/CVD) (Wu et al., 2002) and laser assisted NW growth at elevated temperatures (Duan and Lieber, 2000; Gole et al., 2000; Morales and Lieber, 1998; Wang et al., 1998; Wang et al., 2004) which requires the use of a pulsed laser to ablate a target with gas flowing through the reaction chamber held at elevated temperature. Though proven to produce NWs, the number of variables (heat, vapor, catalyst/substrate type and interfa-

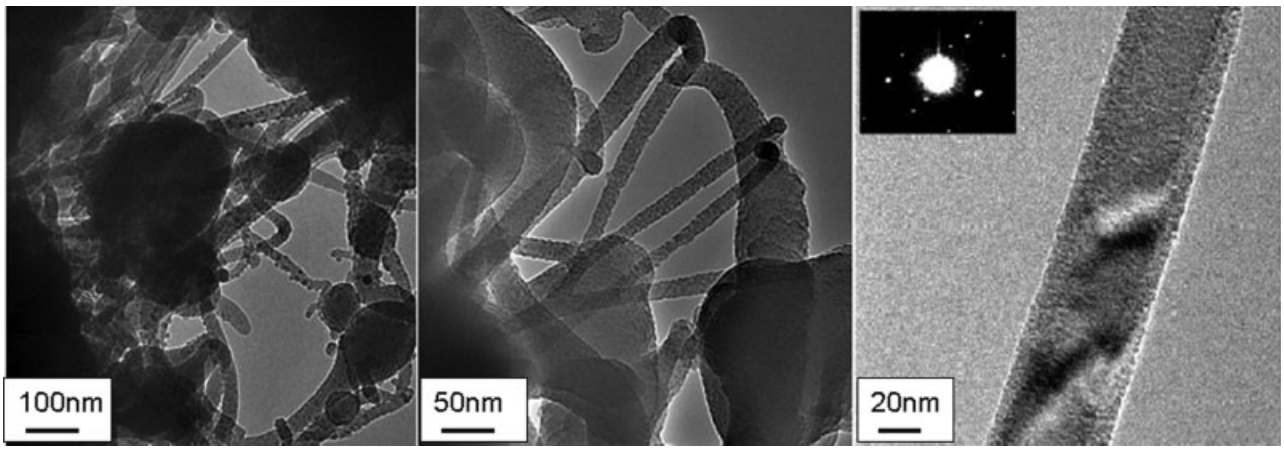

Fig. 3. The drive laser in the DTEM allows for unique synthesis experiments otherwise impossible in conventional in situ TEM, such as laser ablation synthesis of SiO_x (left, middle) and Si (right) nanowires.

cial relationship) involved in the experimental method yields a myriad of different morphologies (Gole et al., 2000; Wang et al., 2004). Though in situ NW growth has been shown in environmental (Kodambaka et al., 2006) and nonenvironmental TEM systems (Stach et al., 2003; Wu and Yang, 2001) with conventional heating methods, laser ablation synthesis of NWs is precluded by direct in situ characterization of the growth procession within the framework of the conventional TEM. Thus, there is a strong need for an experimental method of NW production which allows in situ structural and morphological characterization during laser ablation synthesis of NWs.

In the DTEM, it is possible to produce NWs in situ using pulsed laser ablation with the drive laser. The NW synthesis was performed by exposing an electron transparent target to the pulsed drive laser. For Si NWs, films of Si with a 4 nm Au layer (as a catalyst) were treated with a frequency tripled (355 nm) Nd:YAG laser with 8 ns pulses and laser energies of 240–275μJ (above the ablation threshold) in a 2000 μm^2 laser beam spot size. For SiO_x NWs, films of Si on SiO_2 were treated with the same laser (355 nm Nd: YAG), but at a laser energy of 108 μJ. In a single laser shot, the films yielded oxide-based NWs. The SiO_x and Si NWs are shown in Figure 3. No additional heat or gas was present in the TEM chamber, and thus, modifications in NW growth were produced by varying only one parameter: laser intensity. By controlling the laser intensity, the coated substrates could be melted or ablated to produce NWs. In all cases, the NW production was monitored in situ. Evolution of Si wires during both heating and ablation was monitored in situ using continuous wave (CW) electron beam imaging in the DTEM.

Using the in situ laser drive capabilities of the DTEM, we demonstrate the ability to produce 1D nanostructures under nonequilibrium conditions generated by laser irradiation with simultaneous characterization of their growth. This unique capability opens the door to the development of improved nanoscale fabrication methods and finally, a greater understanding of the growth mechanisms involved in 1D nanostructure production, which could have a tremendous impact on the future use of NWs in electronic devices.

Laser Processing of Polycrystalline Silicon. Another use of the drive laser is to study the role of laser energy on the microstructure of polycrystalline Si grown by laser crystallization for thin film transistor (TFT) applications. Polycrystalline Si (poly-Si) is heavily used in thin film transistors (TFT) for flat panel displays in rapidly growing areas, such as monitors, mobile phones and television (Boyce et al., 1998; Uchikoga and Ibaraki, 2001; Wong et al., 2002). Since electrical properties are closely coupled with microstructure and defect concentration, i.e., the electric activity is governed by defect-induced charge-trapping centers (Brotherton, 1995), it is necessary to understand the origin and role of inter and intragranular defects to better control the device properties. Another concern during processing is grain size. Many studies have shown that larger grain size results in higher electron mobility (Boyce et al., 1998; Brotherton, 1995). Controlling grain size is not the only goal; control over the amount and type of defects (dislocation, twin, and stacking fault concentration) and grain distribution is also important for improving the overall device characteristics (Brotherton, 1995). Typically, in industry, poly-Si films are processed by crystallization of amorphous Si (a-Si) with an excimer laser with pulse durations of <50ns and intensities of a few hundred mJ/cm^2. Crystallization velocities for this type of experiment were previously found to be 10 m/s (Boyce et al., 1998). In our experiments, samples of a-Si/SiO_2 provided by Xerox-PARC were made into an electron transparent film by focused-ion beam (FIB). Because the sample was milled by preferential thinning of the SiO_2/glass side at low ion beam currents (from 0.3 to 0.1 nA for final thinning), we did not find that there was an influence of Ga implantation on the sample. The film was pulsed with the laser to cause melting and crystallization upon supercooling (nucleation and growth occur after melting). Images taken in situ are shown in Figure 4. This capability allows for in situ studies of grain boundary migration and grain size distribution with respect to laser energy and adsorption depth.

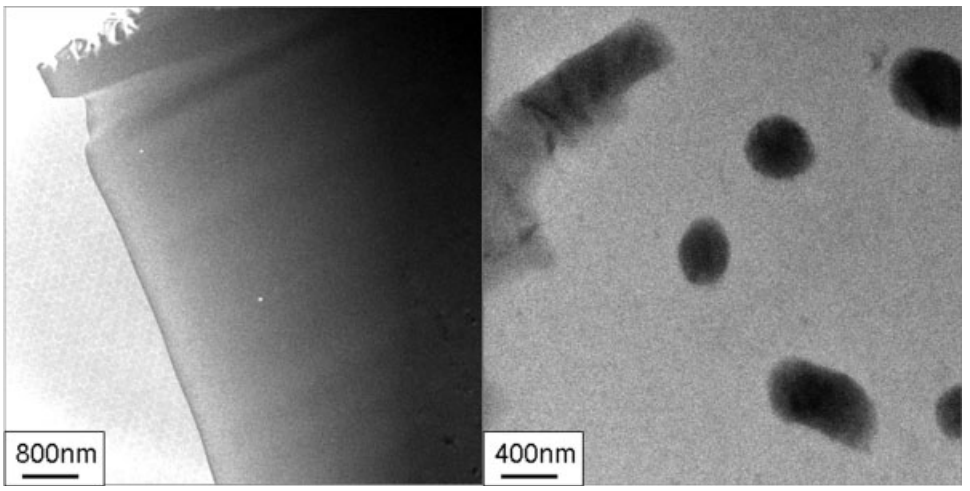

Fig. 4. Plan view images of the crystallization of amorphous silicon. Left image shows 50 nm a-Si on 100 nm SiO_2, before laser processing. Right images shows this same region of material after one laser shot at 108 μJ at 355 nm. Small crystals have nucleated as the laser shot caused melting and crystallization upon supercooling.

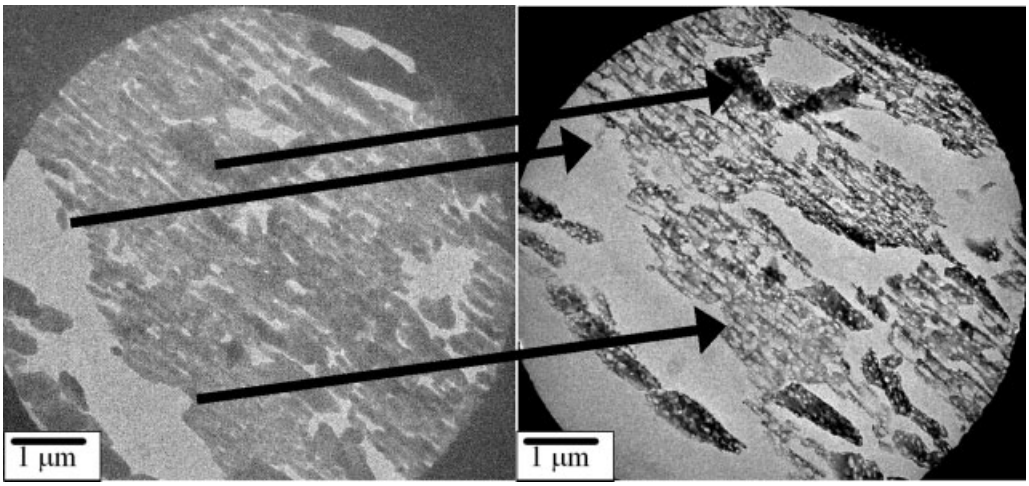

Fig. 5. Attempt to drive the HMX β–δ phase transformation using conventional in situ TEM heating. Illumination conditions were adjusted to minimize the radiation dose to the sample; the circular regions shown constitute the entire electron-illuminated area. Left: Image of sub-μm β-HMX crystals, as prepared (room temperature). Right: Image of roughly the same region (arrows showing corresponding locations, with motion due to thermal drift) after heating to ~150°C.

Circumvention of Competing Processes: HMX transformation

Because of the slow (seconds to minutes) ramp-up times, conventional in situ TEM heating experiments encounter great difficulty in studies of fast, irreversible material processes even under the best of circumstances. But when there exist slow, thermally activated processes that compete with the fast processes of interest, conventional heating studies can become essentially impossible. This difficulty can be avoided by using the rapid, localized heating provided by the DTEM's drive laser.

For example, we recently studied the 170°C β–δ phase transformation (Burnham et al., 2004; Henson et al., 1999, 2002) in the molecular crystal HMX (octahydro-1,3,5,7-tetranitro-1,3,5,7-tetrazocine). Figure 5 shows the results of attempting to drive this transformation with conventional in situ TEM heating using a resistive heating holder in a JEOL 200CX TEM. We found that the material disappeared at a rate estimated to be of order 1 nm/s at 150°C, with a strong dependence on temperature, such that by the time the sample reached the β–δ transformation temperature of 170°C almost all of the material had vanished. Diffraction measurements of the remnants showed no evidence of crystallinity. The image on the right-hand side of Figure 5 is partway through this process, with evident thinning and pock marks across the entire region. Continuous acquisitions of diffraction patterns during this process

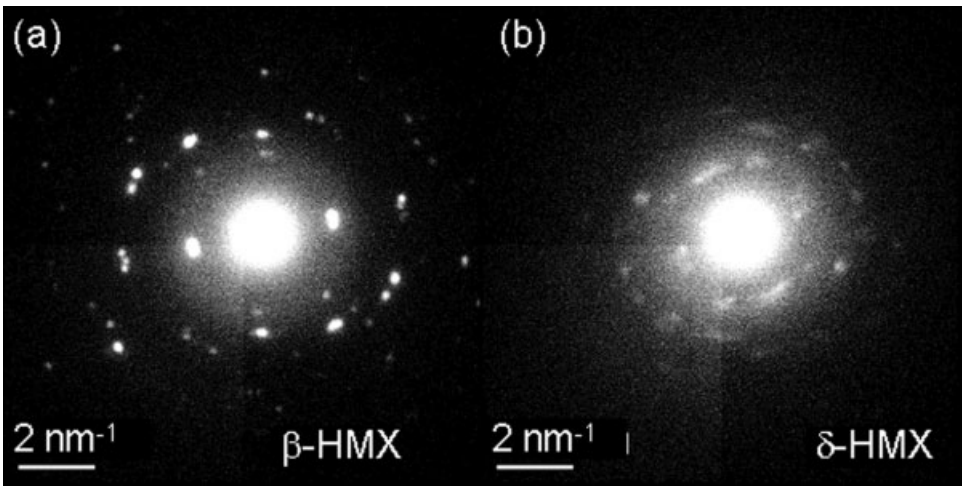

Fig. 6. Diffraction patterns showing the successful driving of the β–δ HMX transformation in the DTEM. (**a**) Coarse-grained β-HMX before application of a laser pulse. (**b**) Fine-grained δ-HMX after the laser pulse and subsequent cooling (increased digital contrast settings).

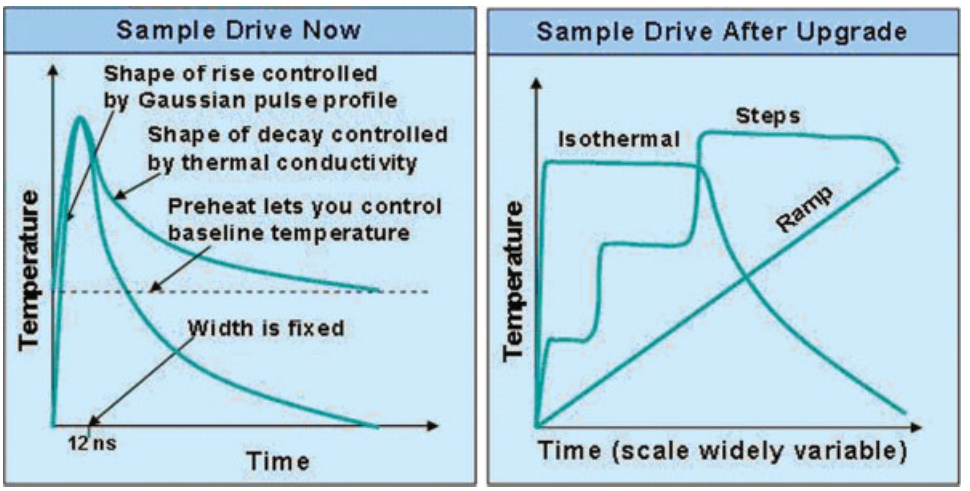

Fig. 7. Comparison of the current drive laser capabilities and the multimode capability after the incorporation of the AWG system. [Color figure can be viewed in the online issue, which is available at www.interscience.wiley.com.]

showed no evidence whatever of the δ phase. Rather, they show an initially strong β phase pattern (similar to that in FIG. 6A) gradually fading into a low-intensity amorphous pattern as the material degraded and vanished.

We recognized that competing processes (including some combination of sublimation, decomposition, and radiation damage from the electron beam) were interfering with our studies of the β–δ transformation. Previous authors (Tappan et al., 2000) have also suggested that it is inherently difficult to drive this transformation in a vacuum, since HMX's volatile decomposition products may play an essential role in destabilizing the β phase.

The DTEM's sample drive laser allowed us to circumvent these problems (Fig. 6). The sample started as sub-μm crystals of β-HMX, with a diffraction pattern as shown in Figure 6A (indexed using the unit cell parameters from (Cady et al., 1963), while the parameters for δ-HMX came from (Cobbledick and Small, 1974). By preheating the sample to 110°C using a conventional heating holder and then using the drive laser to briefly heat a small part of the sample, we were able to keep a small region above the 170°C transition temperature for long enough to nucleate and grow the δ phase in a textured nanocrystalline form which was retained as the sample cooled (Fig. 6B). Since the sample was hot for only a small fraction of a second (estimated ~2 ms, assuming a thermal diffusivity of $\sim 10^{-7}$ m^2/s for the formvar support layer and a drive laser spot diameter of 50 μm), the competing processes that interfered with the conventional experiment (Fig. 5) did not have time to operate. This example shows that the time–temperature profile available in DTEM experiments allows the isolation and study of material processes that are difficult or impossible to study with the slow ramp heating of conventional in situ TEM.

DISCUSSION

It is evident from the results shown in this article that laser-based in situ methods have several unique capabilities that are not available with conventional, resistive heating in situ TEM methods. First and foremost, the maximum allowable temperature of a heating holder is ~1200°C. As shown above, there is virtually no temperature limit of the drive laser. Secondly, the laser can reach a temperature in nanoseconds in a specific region, with no ramp-up time and minimal thermal drift. There is, however, a disadvantage of the drive laser: The sample temperature can only be determined with significant effort. It is necessary to model the absorption characteristics of the laser for each material type and to verify these models with benchmark experiments.

Another limitation of the drive laser is the nanosecond fixed pulse width. Though this short pulse of energy allows for unique and exciting experiments, as outlined above, conventional resistive heating experiments that enable isothermal heating for longer durations are sometimes necessary. Because of this shortcoming, however, a modification of the drive laser is underway. Specifically, the laser system is in the process of being upgraded to a fiber-based amplification system based on a dual arbitrary waveform generator (AWG).

The AWG will enable independent computerized control of both the cathode and the sample drive waveforms, with nanosecond resolution and pulse durations varying from a few nanoseconds to several microseconds. This replaces the present control system in which each laser has a fixed pulsed duration and temporal form. Our ability to control the time–temperature curve at the sample will be greatly improved (Fig. 7). Various profiles, such as ramp-up, progressive heating, and isothermal heating will be possible. The AWG upgrade will allow for parameters for quantitatively measuring phase transition kinetics, surface phenomena, and interface motion. This new system alleviates the disadvantages currently present due to short pulse heating and expands on novel experimental techniques currently possible with a fixed laser pulse width.

Lastly, we are expanding our experimental portfolio beyond current methods to incorporate the use of the drive laser into unique in situ stages for a wide range of sample types and studies. Two of our recent efforts have been the development of an in situ gas stage and an in situ fluid stage. These stages will allow for the study of surface reconstructions in catalysis, in situ chemical vapor deposition nanowire growth studies, and finally, the analysis of biological samples in their natural (un-stained) state. The combination of these distinctive in situ stages and the multimode drive laser opens the door to a wide range of science that is completely inaccessible using any other single technique.

ACKNOWLEDGMENTS

The authors acknowledge the technical assistance of Richard Shuttlesworth and Benjamin Pyke. This work was performed under the auspices of the U.S. Department of Energy, Office of Basic Energy Sciences by Lawrence Livermore National Laboratory under contract DE-AC52-07NA27344.

REFERENCES

Bostanjoglo O. 2002. High speed electron microscopy. In: Hawkes PW, editor. Advanced imaging and electron physics, Vol. 121. New York: Academic Press. p. 1–46.

Bostanjoglo O, Niedrig R, Wedel B. 1994. Ablation of metal films by picosecond laser pusles imaged with high-speed electron microscopy. J Appl Phys 76(5):3045–3048.

Bostanjoglo O, Nink T. 1996. Hydrodynamic instabilities in laser pulsed-produced melts of metal films. J Appl Phys 79(11):8725–8729.

Bostanjoglo O, Weingartner M. 1997. Pulsed photoelectron microscope for imaging laser-induced nanosecond processes. Rev Sci Instrum 68(6):2456–2460.

Bostanjoglo O, Kornitzky J, Tornow RP. 1991. High-speed electron microscopy of laser-induced vaporization of thin films. J Appl Phys 69(4):2581–2583.

Bovin J-O, Wallenberg LR, Smith DJ. 1985. Imaging of atomic clouds outside the surfaces of gold crystals by electron microscopy. Nature 317:47–49.

Boyce JB, Mei P, Fulks RT, Ho J. 1998. Laser processing of polysilicon thin-film transistors: Grain growth and device fabrication. Laser crystallization and modification of semiconductors. Phys Stat Sol (a) 166:729–741.

Brotherton SD. 1995. Topical review: Polycrystalline silicon thin film transistors. Semicond Sci Technol 10:721–738.

Brown MH, Hale KF, Lagneborg R. 1973. Correlation between observed creep behaviour from in-situ experiments in the HVEM and predicted behaviour from the recovery creep theory (high voltage electron microscope examination of Al alloys specimens). Scripta Metall 7:1275.

Burnham AK, Weese RK, Weeks BL. 2004. A distributed activation energy model of thermodynamically inhibited nucleation and growth reactions and its application to the beta-delta phase transition of HMX. J Phys Chem B 108:19432–19441.

Cady HH, Larson AC, Cromer DT. 1963. The crystal structure of a-HMX and a refinement of the structure of b-HMX. Acta Crystallogr 16:617–623.

Caillard D, Martin JL. 1982. Microstructure of alumninum during creep at intermediate temperature. II. *In situ* study of subboundary properties. Acta Metall 30:791–798.

Caillard D, Martin JL. 1983. Microstructure of alumninum during creep at intermediate temperature. III. The rate controlling process. Acta Metall 31:813.

Cobbledick RE, Small R. 1974. The crystal structure of the d-form of 1,3,5,7-tetranitro-1,3,5,7-tetraazacyclooctane (d-HMX). Acta Crystallogr B 30:1918–1922.

Datye AK. 2003. Electron microscopy of catalysts: recent achievements and future prospects. J Catal 216:144–154.

Dömer H, Bostanjoglo O. 2003. High-speed transmission electron microscope. Rev Sci Instrum 74:4369.

Duan X, Lieber CM. 2000. Laser-assisted catalytic growth of single crystal GaN nanowires. J Am Chem Soc 122:188–189.

Gai PL. 2002. Developments in *in situ* environmental cell high-resolution microscopy and applications to catalysis. Top Catal 21(4):161–173.

Gleiter H. 1969. Theory of grain boundary migration rate. Acta Metall 17:565, 853.

Gole JL, Stout JD, Rauch WL, Wang ZL. 2000. Direct synthesis of silicon nanowires. Silica nanospheres, and wire-like nanosphere agglomerates. Appl Phys Lett 76(17):2346.

Hale KF, Butler EP. 1981. Dynamic experiments in the electron microscope. In: Glauert AM, editor. Practical methods in electron microscopy, vol. 9. Amsterdam: North Holland Publishing Company, pp. 239–308.

Henson BF, Smilowitz L, Asay BW, Dickson PM. 2002. The beta-delta phase transition in the energetic nitramine octahydro-1,3,5,7-tetranitro-1,3,5,7-tetrazocine: Thermodynamics. J Chem Phys 117: 3780–3788.

Henson BF, Asay BW, Sander RK, Son SF, Robinson JM, Dickson PM. 1999. Dynamic measurement of the HMX beta-delta phase transition by second harmonic generation. Phys Rev Lett 82:1213–1216.

King WE, Campbell GH, Frank A, Reed B, Schmerge JF, Siwick BJ, Stuart BC, Weber PM. 2005. Ultrafast electron microscopy in materials science, biology, and chemistry. J Appl Phys 97:111101.

King WE, Armstrong M, Malka V, Reed BW, Antoine Rousse A. 2006. Ultrafast imaging of materials: Exploring the gap of space and time. MRS Bull 31:614–619.

Kodambaka S, Hannon JB, Tromp RM, Ross FM. 2006. Control of Si nanowire growth by oxygen. Nano Lett 6(6):1292–1296.

LaGrange T, Campbell GH, Colvin JD, Reed B, King WE. 2006. Nanosecond time resolved electron diffraction studies of the alpha → beta in pure Ti thin films using the dynamic transmission electron microscope (DTEM). J Mater Sci 41:4440–4444.

LaGrange T, Campbell GH, Turchi ,PEA, King WE. 2007. Rapid phase transformation kinetics on a nanoscale: Studies of the alpha → beta transformation in pure, nanocrystalline Ti using the nanosecond dynamic transmission electron microscope. Acta Mater 55:5211–5224.

Lobastov VA, Srinivasan R, Zewail AH. 2005. Four-dimensional ultrafast electron microscopy. Proc Natl Acad Sci USA 102:7069.

Merkle KL, Thompson LJ, Phillpp F. 2004. In-situ HREM studies of grain boundary migration. Interf Sci 12:277–292.

Morales AM, Lieber CM. 1998. A laser ablation method for the synthesis of crystalline semiconductor nanowires. Science 279:208–211.

Rae CMF. 1981. On the movement of grain boundary dislocations in recrystallizing interfaces. Phil Mag A 44:1395.

Rae CMF, Smith DA. 1980. On the mechanisms of grain boundary migration. Phil Mag A 41:477.

Sharma R, Weiss K. 1998. Development of a TEM to study in situ structural and chemical changes at an atomic level during gas–solid interactions at elevated temperatures. Microsc Res Tech 42:270–280.

Sinclair R, Yamashita T, Ponce FA. 1981. Atomic motion on the surface of a cadmium telluride single crystal. Nature 290:386.

Smith DJ, Marks L.D. 1985. Direct imaging of rearrangements on extended gold surfaces. Mater Res Soc Proc 41:129.

Smith DA, Rae CMF, Grovenor CRM. 1980. In: Grain boundary structure and kinetics. Balluffi RW, editor. Metals Park, OH: American Society for Metals. p. 337.

Stach EA, Pauzauskie PJ, Kuykendall T, Goldberger J, He R, Yang P. 2003. Watching GaN nanowires grow. Nano Lett 3(6):867–869.

Taheri ML, Stach E, Radmilovic VR, Weiland H, Rollett AD. 2004. In situ electron microscopy studies of the effect of Zr on grain boundary mobility anisotropy and mobility in an aluminum alloy. Mater Res Soc Symp Proc P7:7.

Tappan AS, Renlund JH, Gieske JH, Miller JC. 2000. Real-time raman spectroscopic and ultrasonic measurements to monitor the HMX beta-delta phase transition and physical changes in thermally damaged energetic materials. In: JANNAF Propulsion Systems Hazards Subcommittee Meeting PSHS-1D-05, Monterey, CA, 2000.

Uchikoga S, Ibaraki N. 2001. Low temperature poly-Si TFT-LCD by excimer laser anneal. Thin Solid Films 383:9–24.

Vogelsang M, Arsenault RJ, Fisher RM. 1986. In situ HVEM study of dislocation generation at Al/SiC interfaces. Metall Trans A 17:379–389.

Wallenberg LR, Bovin J-O, Schmid G. 1985. On the crystal structure of small gold crystals and large gold crystals. Surf Sci 156:256.

Wallenberg LR, Bovin J-O, Petford-Long AK, Smith DJ. 1986. Atomic-resolution study of structural rearrangements in small platinum crystals. Ultramicroscopy 20:71–75.

Wang N, Tang YH, Zhang YF, Lee CS, Lee ST. 1998. Nucleation and growth of Si nanowires from silicon oxide. Phys Rev B 58(24):R16024–R16026.

Wang K, Chung SY, Kim D. 2004. Morphology of Si nanowires fabricated by laser ablation using gold catalysts. Appl Phys A 79:895–897.

Wong WS, Ready S, Matusiak R, White SD, Lu J-P, Street RA. 2002. Amorphous silicon thin-film transistors and arrays fabricated by jet printing. Appl Phys Lett 80(4):610.

Wu Y, Yang P. 2001. Direct observation of vapor-liquid-solid nanowire growth. J Am Chem Soc 123:3165–3166.

Wu Y, Fan R, Yang P. 2002. Block-by-block growth of single-crystalline Si/SiGe superlattice nanowires. Nano Lett 2(2):83–86.

Zewail AH. 2005. Diffraction, crystallography, and microscopy beyond 3D-structural dynamics in space and time. Philos Trans R Soc London A 363:315.